Brief Communication

Increasing frequency and intensity of the most extreme wildfires on Earth

Calum X. Cunningham ⬡ ✉, **Grant J. Williamson** ⬡ **& David M. J. S. Bowman** ⬡

Climate change is exacerbating wildfire conditions, but evidence is lacking for global trends in extreme fire activity itself. Here we identify energetically extreme wildfire events by calculating daily clusters of summed fire radiative power using 21 years of satellite data, revealing that the frequency of extreme events (≥99.99th percentile) increased by 2.2-fold from 2003 to 2023, with the last 7 years including the 6 most extreme. Although the total area burned on Earth may be declining, our study highlights that fire behaviour is worsening in several regions—particularly the boreal and temperate conifer biomes—with substantial implications for carbon storage and human exposure to wildfire disasters.

Extreme wildfires are sporadic features of fire-prone landscapes globally[1], and they carry major ecological, economic and social consequences. Australia's 'Black Summer Bushfires' of 2019 and 2020, for example, were unprecedented in their scale and intensity (measured as radiative power)[2]. These energetically extreme fires released extraordinary quantities of carbon emissions and smoke[3,4], killed an estimated ~2.8 billion vertebrates[5] and burned the entire geographic ranges of 116 plant species[6]. The 2015 wildfires in Indonesia likewise had major social and economic effects: densely populated cities of southeast Asia were blanketed with smog, leading to an estimated 100,000 additional deaths from smoke-related respiratory problems[7] and causing an estimated US$16 billion in direct and indirect economic losses[8].

Most fires on Earth are small[9], ignited by humans[10], and not remarkably damaging. Indeed, fire plays a crucial role in the health of most fire-adapted ecosystems[11]. It has been widely reported that the area burned globally has decreased this century[12–16], but this trend is mostly driven by declines in low-intensity fires in African grasslands and savannas[13,16]. Globally, average fire intensity has also been decreasing this century (with some regional increases)[15], but burn severity, an ecological measure of a fire's immediate effects (for example, biomass loss and mortality), is increasing in more regions than it is decreasing[14].

In contrast to the majority of fires, energetically extreme wildfires are associated with extreme ecological, social and economic consequences[1], including emitting vast quantities of smoke and greenhouse gases that threaten to further accelerate warming[3,4]. Despite their importance, there remains no systematic evidence of temporal trends in extreme wildfires. In a study of energetically extreme wildfires[1], no temporal trend was revealed, potentially because of the relatively short satellite record used in the study (12 years, 2002–2013). Likewise, global trends have not yet been observed for pyrocumulonimbus events (storms triggered by extremely intense wildfires)[17]. A lack of trends is unexpected because warming temperatures and increasing vapour pressure deficit are drying fuels and worsening fire weather across most of the Earth[18–23]. Climate change has already caused fire weather to depart from its historical variability across ~20% of burnable land area globally[24], and recent extremely destructive wildfire seasons have occurred in the Amazon[25], Australia[2], Canada[26], Chile[27], Portugal[28], Indonesia[8], Siberia and the western United States[19,29]. While the notion of increasingly dangerous wildfires pervades the media, such trends have not been systematically shown[30].

Here we use 21 years of satellite observations of the radiative power released by wildfires to evaluate whether energetically extreme wildfire events are increasing in frequency and/or magnitude. We use a similar approach to ref. 1 by calculating the daily summed fire radiative power (FRP; megawatts) of clusters of active fire hotspots observed by the Moderate Resolution Imaging Spectroradiometer (MODIS) and Aqua satellites[31]. To do this, we summed the FRP (ΣFRP) of hotspots in a 0.2° equal-area lattice across the Earth for each of the 7,639 days between 1 January 2003 and 30 November 2023. As distinct from analysing the FRP of individual hotspots, which measure the intensity of a fire at a single time and location, our daily ΣFRP approach characterizes the integrated radiant energy released by broader fire 'events' that may burn concurrently at multiple nearby locations and at multiple time points during the day, thus distinguishing energetically extreme fires from energetically extreme hotspots. This process reduced 88.4 million satellite observations to 30.7 million daily ΣFRP events. We then evaluated temporal trends and biogeographic associations in the most extreme of these events, defined here as those exceeding the 99.99th
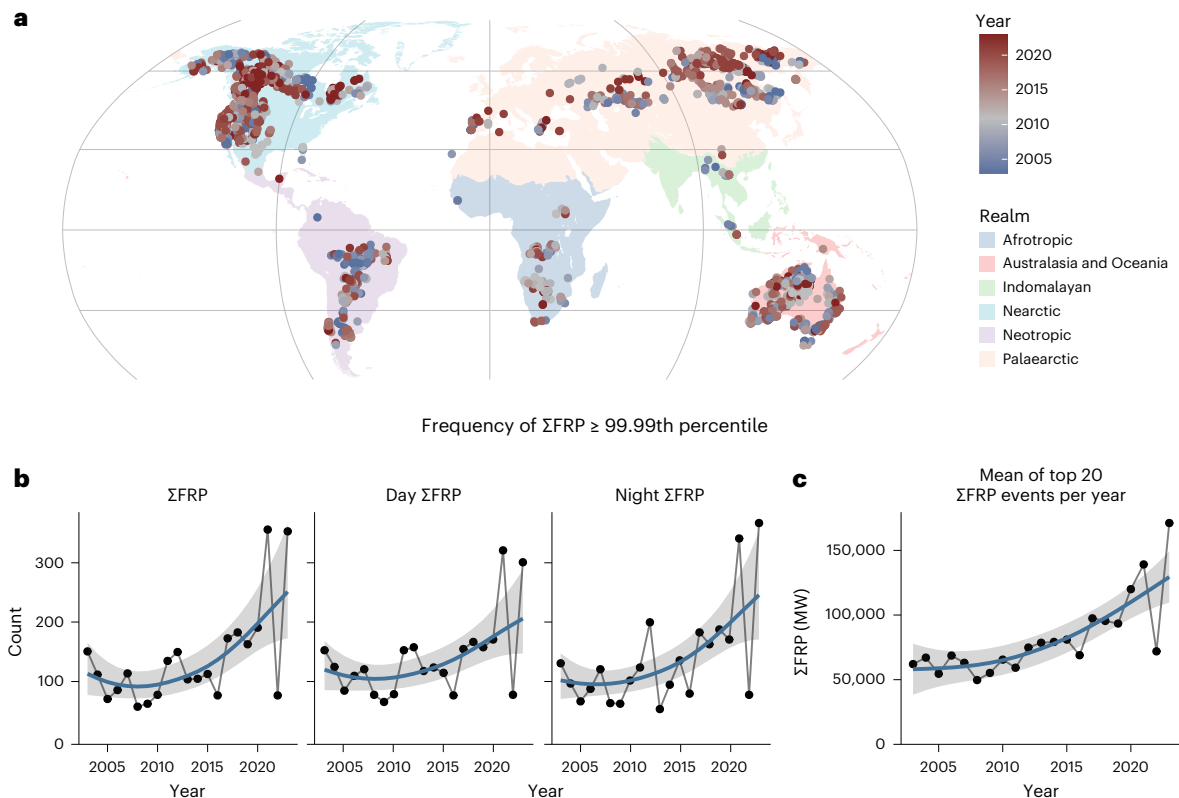
Fire Centre, School of Natural Sciences, University of Tasmania, Hobart, Tasmania, Australia. ✉e-mail: calum.cunningham@utas.edu.au

Fig. 1 | Distribution and trends of the most extreme wildfires on Earth.
The FRP sum (ΣFRP) was calculated by summing the FRP of MODIS hotspots on a 0.2° equal-area lattice for each day from 2003 to 2023. **a**, The points show the locations of the most extreme ΣFRP events, defined as those ≥99.99th percentile, totalling 2,913 events, overlaid on biogeographical realms[34]. See Extended Data Fig. 1 for annual distribution maps. **b**, Extreme wildfire events more than doubled in frequency over the 21 year period, including during both day and night. **c**, The 20 most extreme events in each year show a sustained increase in the average intensity (MW, megawatts) of extreme wildfires. The lines in **b** and **c** show the fit (±95% confidence interval (CI)) of a generalized additive model. Note: values for 2023 do not include December because those data were not available at the time of analysis.

percentile of daily ΣFRP. This process identified 2,913 extreme events (of which 13% were associated with fires burning in the same cell within the subsequent 7 days).

The frequency of extreme wildfire events increased by a model-estimated 2.2-fold over the 21-year study period (Fig. 1b; $P_{f(year)} = 0.00003$, estimated degrees of freedom (edf) = 2, χ^2 statistic = 18.4). Extreme events occurred on all continents except Antarctica (Fig. 1a and Extended Data Fig. 1). The six most extreme years with respect to the frequency of major events occurred from 2017 onwards (Fig. 1b). This increasing trend was apparent for ΣFRP calculated using day and night hotspots separately (Fig. 1b), but there was stronger statistical evidence of an increasing trend at night-time ($P_{f(year)} = 0.00006$, edf = 1.84, χ^2 = 16.65) than at daytime ($P_{f(year)} = 0.003$, edf = 1.68, χ^2 = 8.98). The stronger increasing trend at night is in line with the observation that temperatures are warming faster at night than during the day[32], and such warming is consequently reducing the night-time barrier to wildfire[33].

In addition to the increasing frequency of extreme wildfire events, the magnitude of extreme wildfire events has also increased significantly. For the 20 most extreme events in each year, the average ΣFRP has similarly increased by 2.3-fold over the study, and this increase appears to be accelerating (Fig. 1c; $P_{f(year)} = 0.00003$, edf = 1.96, F statistic = 3.88). Like the frequency of extreme events, the 6 most extreme years with respect to magnitude occurred within the last 7 years (Fig. 1c).

Relative to the area occupied by the Earth's biogeographic realms and biomes, extreme events were disproportionately concentrated in the Nearctic and Australasia/Oceania realms (ratios > 1; Fig. 2a)[34]

and in the temperate conifer forest, Mediterranean forest/woodland, and boreal forest biomes (Fig. 2b). Biome-specific generalized linear models revealed that the global increase in extreme events was almost entirely driven by strong increases in the temperate conifer forest biome ($P_{year} = 0.00002$, z statistic = 4.28) and the boreal forests and taiga biome (Fig. 2c; $P_{year} = 0.000003$, z = 4.64). In the temperate conifer forest biome, the annual number of extreme events estimated by a generalized linear model increased by 11.1-fold, from 6 in 2003 to 67 in 2023 (Fig. 2c). Similarly, extreme events in the boreal forest biome increased by 7.3-fold, from a model-estimated 14.9 to 108.7, over the 21 years of the study (Fig. 2c). No significant trends were apparent in other biomes (Fig. 2c). The increasing trends in the boreal forest and temperate conifer forest biomes are in line with documented increases in mean FRP in those regions[15].

The frequency of extreme events has increased exponentially in the temperate conifer forests of the American West and the boreal forest of North America and Russia (Fig. 2c). Recent extreme fire years in the western United States have been characterized by extremely low fuel moisture over very broad areas[35]. Such increasing fuel aridity has been linked to an exponential increase in burned area because aridity promotes fire growth, and the potential for rapid growth increases as fires get larger[36]. Increasing fuel aridity caused by anthropogenic climate change has driven more than half of the increase in the extent of forest fire in the western United States between 1979 and 2015[23], and simulations suggest that fuel limitations from fire-fuel feedbacks are unlikely to significantly quell the trajectory[37]. Similar trends between anomalous area burnt and fuel dryness have also been observed in southeast Australia[2,19].
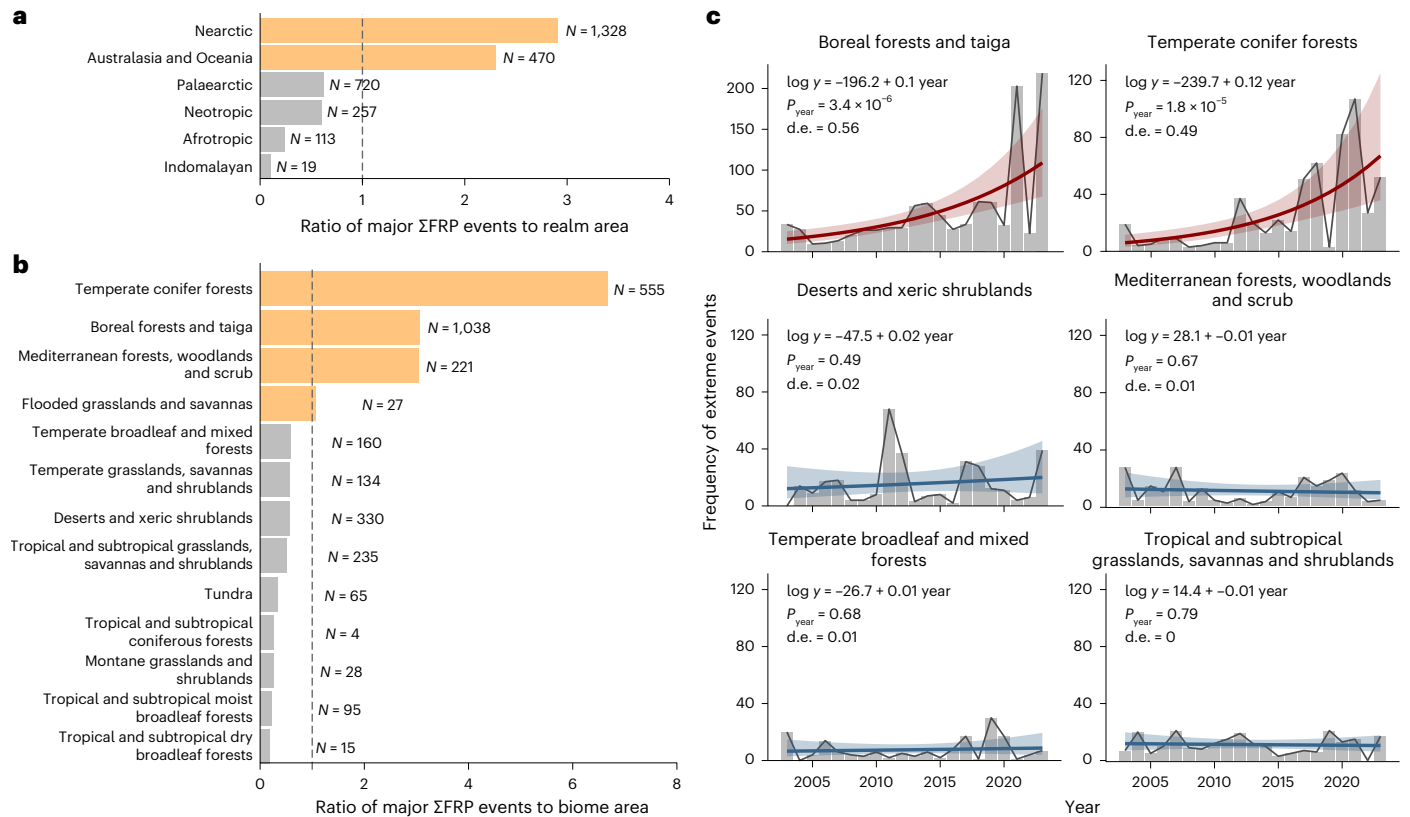
Fig. 2 | Patterns in extreme wildfire events among biogeographical realms and biomes. a,b, Ratio of extreme events to the area of the biogeographical realms (**a**) and biomes (**b**). Ratios were calculated by dividing the proportion of extreme events occurring in a realm or biome by the proportional area occupied by a realm or biome, with ratios >1 indicating a disproportionately high rate of extreme events (coloured orange). *N* indicates the number of extreme events. Biogeographical realms are shown in Fig. 1a, and biomes are shown in

Supplementary Fig. 2, as delineated by ref. 34. **c**, Trends in the frequency of events among biomes with the most extreme events. The lines denote the fit (±95% CI) of generalized linear models, with annotations showing the model formula, *P* value for 'year' and deviance explained ('d.e.'). These regressions indicate that the overall increase in extreme events is strongly driven by increases in the temperate conifer and boreal forest biomes. Note: a different *y*-axis is used for the boreal forest and taiga biome.

Despite the importance of extreme wildfire events, research has not yet, to our knowledge, revealed global trends in frequency or magnitude[19]. This is probably due in part to the relatively short period over which satellites have observed FRP[1]. Short time series (9 years, 2013–2021) have similarly impeded the discovery of trends in extreme fire-induced pyrocumulonimbus storms[17], but a lack of evidence due to data deficiencies does not imply an absence of trends.

The previous lack of documented trends in extreme wildfires also probably stems from the dominant focus of the literature on burned area. Many studies, for example, report that the global burned area has decreased this century (for example, refs. 12–16), leading policy commentators to question the reality of worsening wildfire disasters (for example, ref. 38). Yet, as most fires are human ignited and have relatively small impacts, a focus on average intensities and global burned area means that such analyses are swamped by relatively low-impact fires, including fire used for habitat management, pastoralism, agriculture and silviculture[39,40]. A focus on global averages disproportionately weights Africa (67% of burned area) and conceals opposing trends in different regions[16]. Importantly, a focus on average intensities obscures the extreme events—those that cause the most damage and release the most emissions. By characterizing the daily integrated radiant energy released by fires, we contend that the ΣFRP approach used here provides a vital measure of the way in which fire behaviour is responding to climate change.

Our results show that events of extreme intensity have more than doubled in frequency and magnitude, with increases largely concentrated in the carbon-rich[41] boreal and temperate conifer forests of the

northern hemisphere. There were also several foci of extreme events in the southern hemisphere (southern Africa, Australia and South America). The last 7 years included the six most extreme years for energetically extreme wildfires. The most recent year (2023) had both the hottest global temperature on record[42] and the most extreme wildfire intensities (Fig. 1c) since MODIS sensors began observing wildfires. The increasing frequency and magnitude of extreme wildfire events is in step with global heating, highlighting the urgency with which we must adapt to a climate that is more conducive to extreme wildfires.

Methods

Identifying energetically extreme wildfire events

The MODIS sensors on NASA's Terra and Aqua satellites identify active wildfires based on thermal anomalies. The MCD14ML product[43] provides point locations of wildfire 'hotspots' at a resolution of 1 km. These locations represent the centre of a 1 km pixel that was identified by the fire and thermal anomaly algorithm as containing at least one fire somewhere within the pixel, thus detecting fires substantially smaller than a pixel[44]. We excluded locations labelled as probably resulting from non-fire sources, such as volcanoes, other static sources or offshore (for example, industrial). For additional robustness, we further filtered out 'low confidence' fires (that is, confidence <30 (ref. 45)). Each fire observation is accompanied by a measure of FRP, measuring the instantaneous fire energy (megawatts) emitted by a fire, which is known to scale to smoke plume size[46] and has been widely used as a proxy of fire intensity[1]. The Terra satellite provides daily equatorial overpasses at approximately 10:30 a.m. and 10:30 p.m., and the Aqua

satellite at 1:30 a.m. and 1:30 p.m., allowing separate investigations of trends in daytime and night-time fires.

Polar-orbiting satellites are biased at high latitudes because there is some overlap in the swaths of adjacent satellite overpasses[47], leading to the possibility that the same pixel is double counted in subsequent orbits. We corrected this problem by identifying and omitting likely duplicate hotspots, similar to the approach of a previous study[48]. For the Terra and Aqua satellites, there should each be a maximum of one hotspot for each day and each night in each pixel. Thus, to identify likely duplicates, we identified pixels with multiple observations in a given day or night at a resolution of 500 m. Such cases with multiple hotspots indicate a likely duplicate, in which cases we retained one hotspot at random, leaving a combined maximum of four hotspots per 24 h period in each location. Of a total dataset of 88.4 million hotspots, this cleaning process removed 176,181 (0.19%) likely duplicates.

The Terra satellite began collecting data in February 2000[44] but suffered from hardware problems before November 2000[45]. The Aqua satellite was launched later and began collecting data in June 2002[44]. We chose to analyse the full combined Terra and Aqua datasets to provide the fullest characterization of fires over the course of a day. Thus, because of the lower sampling effort before 2003, we based our primary analysis on the years 2003–2023. However, see Supplementary Fig. 1 for a comparison of the trends shown by Terra (2001–2023) and Aqua (2003–2023), revealing similar trends in both satellites.

To identify energetically extreme wildfire events, we calculated the daily energy released by wildfires using an equal-area, equal-shape global lattice with a 0.2° resolution, equating to cell sizes of approximately 22 × 22 km (~495 km^2). We selected this scale as an ecologically reasonable but computationally tractable scale for analysing large volumes of daily satellite data at a global scale. For each cell, we summed the FRP (ΣFRP) of hotspots for each of the 7,639 days between 1 January 2003 and 30 November 2023. At the time of writing, scientific-quality observations were not yet available for December 2023, thus providing a partial and conservative record of the number of extreme events in 2023. This process yielded 30.7 million daily ΣFRP 'events' from 88.4 million hotspot observations. Because it has been reported that global warming is leading to warmer and drier air at night, in turn weakening the night-time barrier to fire[33], we repeated the ΣFRP aggregation process for daytime and night-time fires separately to investigate whether trends differed during day and night.

After calculating the ΣFRP events, we then selected the most energetically extreme events for subsequent analysis, defined here as events with ΣFRP ≥ 99.99th percentile (N = 2,913 events). Although this threshold itself is arbitrary, it unambiguously captures fires of extreme integrated radiant power output, does so in a systematic and unbiased fashion, and yields a reasonable sample size for subsequent analyses. All analyses were conducted using R version 4.3.0 (ref. [49]).

Temporal and biogeographic trends in extreme wildfires

To characterize the biogeographic patterns in extreme events, we calculated the area-normalized ratio of extreme events among the biogeographical realms and biomes of the Earth. Biogeographical realms and biomes are described in ref. [34]. To calculate the ratio, we divided the proportion of extreme events occurring in each realm and biome by the proportion of the Earth's land area occupied by those regions (excluding Antarctica). If extreme events occurred randomly, we would expect ratios of approximately one; values substantially larger than one indicate extreme events are disproportionately common, and values less than one indicate extreme events are disproportionately rare.

To evaluate temporal trends in the frequency and magnitude of extreme events, we fit separate statistical models that investigate (1) the frequency of extreme events globally, (2) the frequency of extreme events among biomes and (3) the magnitude of extreme events globally. In all models, we interpreted *P* values as continuous rather than categorical measures of the strength of evidence, as previously advocated[50].

First, we fit a generalized additive model (GAM) of the annual count of extreme events in response to a smooth (that is, nonlinear) effect of year (continuous variable; 2003–2023)[51]. GAMs allow fitting of nonlinear effects if supported by the data. We fit the model using automatic term selection ('select = TRUE') available in the 'mgcv' package[51], which imposes an additional penalty on smooth terms such that they are penalized out of the model if there is little evidence for an effect. We fit the model using the negative binomial distribution to account for overdispersion[52]. We followed the same process to model the trend for day ΣFRP and night ΣFRP separately.

Second, we fit separate generalized linear models for each of the six biomes with the largest number of events (providing a reasonable sample to interrogate for trends). We fit these models with the annual count of extreme events modelled in response to a fixed effect of year, using the negative binomial distribution to account for overdispersion[52].

Third, to investigate trends in the magnitude of the most extreme events, we selected the 20 most extreme events from each year, from which we calculated the annual average of extreme ΣFRP. We then modelled the annual average of extreme ΣFRP in response to a nonlinear effect of 'year' using a GAM with Gaussian distribution. Generalized linear models and GAMs were fit using the 'mgcv' package (version 1.8–42)[51].

Reporting summary
Further information on research design is available in the Nature Portfolio Reporting Summary linked to this article.

Data availability
MODIS active fire records used in the analysis were downloaded from the University of Maryland ftp server (sftp://fuoco.geog.umd.edu) and are available via figshare at https://doi.org/10.6084/m9.figshare.25132151 (ref. [53]). Biomes of the world were downloaded from https://ecoregions.appspot.com/.

Code availability
Code for the analysis is available via figshare at https://doi.org/10.6084/m9.figshare.25687113 (ref. [54]).

References
1. Bowman, D. M. J. S. et al. Human exposure and sensitivity to globally extreme wildfire events. *Nat. Ecol. Evol.* **1**, 0058 (2017).
2. Abram, N. J. et al. Connections of climate change and variability to large and extreme forest fires in southeast Australia. *Commun. Earth Environ.* **2**, 8 (2021).
3. Johnston, F. H. et al. Unprecedented health costs of smoke-related PM$_{2.5}$ from the 2019–20 Australian megafires. *Nat. Sustain.* **4**, 42–47 (2021).
4. van der Velde, I. R. et al. Vast CO$_2$ release from Australian fires in 2019–2020 constrained by satellite. *Nature* **597**, 366–369 (2021).
5. van Eeden, L. M. & Dickman, C. R. in *Australia's Megafires: Biodiversity Impacts and Lessons from 2019–2020* (eds Rumpff, L. et al) Ch. 12 (CSIRO Publishing, 2023).
6. Godfree, R. C. et al. Implications of the 2019–2020 megafires for the biogeography and conservation of Australian vegetation. *Nat. Commun.* **12**, 1023 (2021).
7. Koplitz, S. N. et al. Public health impacts of the severe haze in Equatorial Asia in September–October 2015: demonstration of a new framework for informing fire management strategies to reduce downwind smoke exposure. *Environ. Res. Lett.* **11**, 094023 (2016).
8. The World Bank *The Cost of Fire: An Economic Analysis of Indonesia's 2015 Fire Crisis* (World Bank, 2016).
9. Archibald, S., Lehmann, C. E. R., Gómez-Dans, J. L. & Bradstock, R. A. Defining pyromes and global syndromes of fire regimes. *Proc. Natl Acad. Sci. USA* **110**, 6442–6447 (2013).

10. Balch, J. K. et al. Human-started wildfires expand the fire niche across the United States. *Proc. Natl Acad. Sci. USA* **114**, 2946–2951 (2017).

11. Bowman, D. M. J. S. et al. Fire in the Earth system. *Science* **324**, 481–484 (2009).

12. Zheng, B. et al. Increasing forest fire emissions despite the decline in global burned area. *Sci. Adv.* https://doi.org/10.1126/sciadv.abh2646 (2021).

13. Andela, N. et al. A human-driven decline in global burned area. *Science* **356**, 1356–1362 (2017).

14. Fernández-García, V. & Alonso-González, E. Global patterns and dynamics of burned area and burn severity. *Remote Sens.* **15**, 3401 (2023).

15. Yang, X., Zhao, C., Zhao, W., Fan, H. & Yang, Y. Characterization of global fire activity and its spatiotemporal patterns for different land cover types from 2001 to 2020. *Environ. Res.* **227**, 115746 (2023).

16. Zubkova, M., Humber, M. L. & Giglio, L. Is global burned area declining due to cropland expansion? How much do we know based on remotely sensed data? *Int. J. Remote Sens.* **44**, 1132–1150 (2023).

17. Fromm, M., Servranckx, R., Stocks, B. J. & Peterson, D. A. Understanding the critical elements of the pyrocumulonimbus storm sparked by high-intensity wildland fire. *Commun. Earth Environ.* **3**, 243 (2022).

18. Jain, P., Castellanos-Acuna, D., Coogan, S. C. P., Abatzoglou, J. T. & Flannigan, M. D. Observed increases in extreme fire weather driven by atmospheric humidity and temperature. *Nat. Clim. Change* **12**, 63–70 (2022).

19. Bowman, D. M. J. S. et al. Vegetation fires in the Anthropocene. *Nat. Rev. Earth Environ.* **1**, 500–515 (2020).

20. Zhuang, Y., Fu, R., Santer, B. D., Dickinson, R. E. & Hall, A. Quantifying contributions of natural variability and anthropogenic forcings on increased fire weather risk over the western United States. *Proc. Natl Acad. Sci. USA* **118**, e2111875118 (2021).

21. Novick, K. A. et al. The impacts of rising vapour pressure deficit in natural and managed ecosystems. *Plant Cell Environ.* https://doi.org/10.1111/pce.14846 (2024).

22. Ellis, T. M., Bowman, D. M. J. S., Jain, P., Flannigan, M. D. & Williamson, G. J. Global increase in wildfire risk due to climate-driven declines in fuel moisture. *Glob. Change Biol.* **28**, 1544–1559 (2022).

23. Abatzoglou, J. T. & Williams, A. P. Impact of anthropogenic climate change on wildfire across western US forests. *Proc. Natl Acad. Sci. USA* **113**, 11770–11775 (2016).

24. Abatzoglou, J. T., Williams, A. P. & Barbero, R. Global emergence of Anthropogenic climate change in fire weather indices. *Geophys. Res. Lett.* **46**, 326–336 (2019).

25. Silveira, M. V. F., Silva-Junior, C. H. L., Anderson, L. O. & Aragão, L. E. O. C. Amazon fires in the 21st century: the year of 2020 in evidence. *Glob. Ecol. Biogeogr.* **31**, 2026–2040 (2022).

26. Parisien, M.-A. et al. Abrupt, climate-induced increase in wildfires in British Columbia since the mid-2000s. *Commun. Earth Environ.* **4**, 309 (2023).

27. Bowman, D. M. et al. Human–environmental drivers and impacts of the globally extreme 2017 Chilean fires. *Ambio* **48**, 350–362 (2019).

28. Turco, M. et al. Climate drivers of the 2017 devastating fires in Portugal. *Sci. Rep.* **9**, 13886 (2019).

29. Iglesias, V., Balch, J. K. & Travis, W. R. U.S. fires became larger, more frequent, and more widespread in the 2000s. *Sci. Adv.* **8**, eabc0020 (2022).

30. Doerr, S. H. & Santín, C. Global trends in wildfire and its impacts: perceptions versus realities in a changing world. *Philos. Trans. R. Soc. B* **371**, 20150345 (2016).

31. Giglio, L., Schroeder, W., Hall, J. & Justice, C. *MODIS Collection 6 Active Fire Product User's Guide Revision B* (NASA, 2018); https://modis-fire.umd.edu/files/MODIS_C6_Fire_User_Guide_B.pdf

32. Easterling, D. R. et al. Maximum and minimum temperature trends for the globe. *Science* **277**, 364–367 (1997).

33. Balch, J. K. et al. Warming weakens the night-time barrier to global fire. *Nature* **602**, 442–448 (2022).

34. Dinerstein, E. et al. An ecoregion-based approach to protecting half the terrestrial realm. *BioScience* **67**, 534–545 (2017).

35. Abatzoglou, J. T., Rupp, D. E., O'Neill, L. W. & Sadegh, M. Compound extremes drive the Western Oregon wildfires of September 2020. *Geophys. Res. Lett.* **48**, e2021GL092520 (2021).

36. Juang, C. S. et al. Rapid growth of large forest fires drives the exponential response of annual forest-fire area to aridity in the Western United States. *Geophys. Res. Lett.* **49**, e2021GL097131 (2022).

37. Abatzoglou, J. T. et al. Projected increases in western US forest fire despite growing fuel constraints. *Commun. Earth Environ.* **2**, 227 (2021).

38. Lomborg, B. Climate change hasn't set the world on fire. *Wall Street Journal* (31 June 2023).

39. Le Page, Y., Oom, D., Silva, J. M. N., Jönsson, P. & Pereira, J. M. C. Seasonality of vegetation fires as modified by human action: observing the deviation from eco-climatic fire regimes. *Glob. Ecol. Biogeogr.* **19**, 575–588 (2010).

40. Bowman, D. M. J. S. et al. The human dimension of fire regimes on Earth. *J. Biogeogr.* **38**, 2223–2236 (2011).

41. Schimel, D. et al. Observing terrestrial ecosystems and the carbon cycle from space. *Glob. Change Biol.* **21**, 1762–1776 (2015).

42. Witze, A. Earth boiled in 2023—will it happen again in 2024? *Nature News* (12 January 2024); https://www.nature.com/articles/d41586-024-00074-z

43. MODIS Collection 6 Hotspot/Active Fire Detections MCD14ML distributed from NASA FIRMS; https://doi.org/10.5067/FIRMS/MODIS/MCD14ML

44. Giglio, L., Descloitres, J., Justice, C. O. & Kaufman, Y. J. An enhanced contextual fire detection algorithm for MODIS. *Remote Sens. Environ.* **87**, 273–282 (2003).

45. Giglio, L., Schroeder, R. L., Hall, J. V. & Justice, C. *MODIS Collection 6 and Collection 6.1 Active Fire Product User's Guide* (NASA, 2021).

46. Williamson, G. J., Price, O. F., Henderson, S. B. & Bowman, D. M. J. S. Satellite-based comparison of fire intensity and smoke plumes from prescribed fires and wildfires in south-eastern Australia. *Int. J. Wildland Fire* **22**, 121–129 (2013).

47. Giglio, L., Csiszar, I. & Justice, C. O. Global distribution and seasonality of active fires as observed with the Terra and Aqua Moderate Resolution Imaging Spectroradiometer (MODIS) sensors. *J. Geophys. Res. Biogeosci.* https://doi.org/10.1029/2005JG000142 (2006).

48. Korontzi, S., McCarty, J., Loboda, T., Kumar, S. & Justice, C. Global distribution of agricultural fires in croplands from 3 years of Moderate Resolution Imaging Spectroradiometer (MODIS) data. *Glob. Biogeochem. Cycles* https://doi.org/10.1029/2005GB002529 (2006).

49. R Core Team. *R: A Language and Environment for Statistical Computing* (R Foundation for Statistical Computing, 2023); https://www.r-project.org/

50. Muff, S., Nilsen, E. B., O'Hara, R. B. & Nater, C. R. Rewriting results sections in the language of evidence. *Trends Ecol. Evol.* https://doi.org/10.1016/j.tree.2021.10.009 (2021).

51. Wood, S. N. *Generalized Additive Models: An Introduction with R* 2nd edn (CRC Press, 2017).

52. Lindén, A. & Mäntyniemi, S. Using the negative binomial distribution to model overdispersion in ecological count data. *Ecology* **92**, 1414–1421 (2011).

53. Cunningham, C. MODIS active fire records used in analysis of extreme wildfires. *figshare* https://doi.org/10.6084/m9.figshare.25132151.v1 (2024).
54. Cunningham, C. Code accompanying "Increasing frequency and intensity of the most extreme wildfires on Earth". *figshare* https://doi.org/10.6084/m9.figshare.25687113.v1 (2024).

Author contributions
C.X.C.: formal analysis, investigation, methodology, software, visualization, and writing—original draft, review and editing. G.J.W.: conceptualization, methodology, and writing—review and editing. D.M.J.S.B.: conceptualization, funding acquisition, project administration, supervision, and writing—review and editing.

Competing interests
The authors declare no competing interests.

Additional information
Extended data is available for this paper at https://doi.org/10.1038/s41559-024-02452-2.

Supplementary information The online version contains supplementary material available at https://doi.org/10.1038/s41559-024-02452-2.

Correspondence and requests for materials should be addressed to Calum X. Cunningham.

Peer review information *Nature Ecology & Evolution* thanks Evan Ellicott and Helen Poulos for their contribution to the peer review of this work. Peer reviewer reports are available.

Reprints and permissions information is available at www.nature.com/reprints.

Extended Data Fig. 1 | Global distribution of extreme wildfire events in each year from 2003 to 2023. Points show the locations of energetically extreme events in each year (≥ 99.99th percentile).

nature portfolio

Corresponding author(s): Calum X Cunningham

Last updated by author(s): Apr 29, 2024

Reporting Summary

Nature Portfolio wishes to improve the reproducibility of the work that we publish. This form provides structure for consistency and transparency in reporting. For further information on Nature Portfolio policies, see our Editorial Policies and the Editorial Policy Checklist.

Statistics

For all statistical analyses, confirm that the following items are present in the figure legend, table legend, main text, or Methods section.

n/a	Confirmed	
☐	☒	The exact sample size (*n*) for each experimental group/condition, given as a discrete number and unit of measurement
☐	☒	A statement on whether measurements were taken from distinct samples or whether the same sample was measured repeatedly
☐	☒	The statistical test(s) used AND whether they are one- or two-sided *Only common tests should be described solely by name; describe more complex techniques in the Methods section.*
☐	☒	A description of all covariates tested
☒	☐	A description of any assumptions or corrections, such as tests of normality and adjustment for multiple comparisons
☐	☒	A full description of the statistical parameters including central tendency (e.g. means) or other basic estimates (e.g. regression coefficient) AND variation (e.g. standard deviation) or associated estimates of uncertainty (e.g. confidence intervals)
☐	☒	For null hypothesis testing, the test statistic (e.g. *F*, *t*, *r*) with confidence intervals, effect sizes, degrees of freedom and *P* value noted *Give P values as exact values whenever suitable.*
☒	☐	For Bayesian analysis, information on the choice of priors and Markov chain Monte Carlo settings
☒	☐	For hierarchical and complex designs, identification of the appropriate level for tests and full reporting of outcomes
☐	☒	Estimates of effect sizes (e.g. Cohen's *d*, Pearson's *r*), indicating how they were calculated

Our web collection on statistics for biologists contains articles on many of the points above.

Software and code

Policy information about availability of computer code

Data collection	No specialized software were used by the authors for data collection.
Data analysis	Code for the analysis is available at http://doi.org/10.6084/m9.figshare.25687113. To identify energetically extreme wildfire events, we calculated the daily energy released by wildfires using an equal area, equal shape global lattice with a 0.2° resolution, equating to cell sizes of approximately 22 × 22 km (~495km2). For each cell, we summed the FRP (ΣFRP) of hotspots for each of the 7,639 days between 1 Jan 2003 and 30 Nov 2023. This process yielded 30.7-million daily ΣFRP "events" from 88.4-million satellite observations. After calculating ΣFRP events, we then selected the most energetically extreme events for subsequent analysis, defined here as events with ΣFRP ≥ 99.99th percentile (N = 2,913 events). To evaluate temporal trends in the frequency and magnitude of extreme events, we fitted separate statistical models that investigate (i) the frequency of extreme events globally, (ii) the frequency of extreme events among biomes, and (iii) the magnitude of extreme events globally. In all models, we interpreted p-values as continuous rather than categorical measures of the strength of the evidence. First, we fitted a generalised additive model (GAM) of the annual count of extreme events in response to a smooth (i.e., non-linear) effect of year (continuous variable; 2003-2023). GAMs allow fitting of non-linear effects if supported by the data. We fitted the model using automatic term selection ("select = TRUE") available in the "mgcv" package, which imposes an additional penalty on smooth terms such that they are penalised out of the model if there is little evidence for an effect. We fitted the model using the negative binomial distribution to account for overdispersion. We followed the same process to model the trend for day ΣFRP and night ΣFRP separately.

Second, we fitted separate generalised linear models (GLM) for each of the 6 biomes with the largest number of events (providing a reasonable sample to interrogate for trends). We fitted these models with the annual count of extreme events modelled in response to a fixed effect of year, using the negative binomial distribution to account for overdispersion.

Third, to investigate trends in the magnitude of the most extreme events, we selected the 20 most extreme events from each year, from which we calculated the annual average of extreme ΣFRP. We then modelled the annual average of extreme ΣFRP in response to a non-linear effect of "year" using a GAM with Gaussian distribution.

All analyses were conducted using R version 4.3.0. GAMs and GLMs were fit using the "mgcv" package (version 1.8-42).

For manuscripts utilizing custom algorithms or software that are central to the research but not yet described in published literature, software must be made available to editors and reviewers. We strongly encourage code deposition in a community repository (e.g. GitHub). See the Nature Portfolio guidelines for submitting code & software for further information.

Data

Policy information about availability of data

All manuscripts must include a data availability statement. This statement should provide the following information, where applicable:
- Accession codes, unique identifiers, or web links for publicly available datasets
- A description of any restrictions on data availability
- For clinical datasets or third party data, please ensure that the statement adheres to our policy

MODIS active fire records used in the analysis were downloaded from the University of Maryland ftp server (sftp://fuoco.geog.umd.edu) and archived at https://figshare.com/s/1de93c198fa2e15150da. Biomes of the world were downloaded from https://ecoregions.appspot.com/

Research involving human participants, their data, or biological material

Policy information about studies with human participants or human data. See also policy information about sex, gender (identity/presentation), and sexual orientation and race, ethnicity and racism.

Reporting on sex and gender	N/A
Reporting on race, ethnicity, or other socially relevant groupings	N/A
Population characteristics	N/A
Recruitment	N/A
Ethics oversight	N/A

Note that full information on the approval of the study protocol must also be provided in the manuscript.

Field-specific reporting

Please select the one below that is the best fit for your research. If you are not sure, read the appropriate sections before making your selection.

☐ Life sciences   ☐ Behavioural & social sciences   ☒ Ecological, evolutionary & environmental sciences

For a reference copy of the document with all sections, see nature.com/documents/nr-reporting-summary-flat.pdf

Ecological, evolutionary & environmental sciences study design

All studies must disclose on these points even when the disclosure is negative.

Study description	The study analysed the intensity of the most extreme wildfires on Earth over 21 years.
Research sample	We analysed a global, systematic sample of active wildfires observed by NASA's MODIS satellites. Our primary analysis used data from the Terra and Aqua satellites between Jan 2003 and Nov 2023.
Sampling strategy	We used all data available from the MODIS Terra and Aqua satellites between Jan 2003 and Nov 2023 (but see "Data exclusions").
Data collection	The Moderate Resolution Imaging Spectroradiometer (MODIS) sensors on NASA's Terra and Aqua satellites identify active wildfires based on thermal anomalies. The MCD14ML product provides point locations of predicted wildfires at a resolution of 1 km. These locations represent the centre of a 1 km pixel that was identified by the fire and thermal anomalies algorithm as containing at least one fire somewhere within the pixel, thus detecting fires significantly smaller than a pixel. Each fire observation is accompanied by a measure of fire radiative power (FRP), measuring the radiative energy (megawatts) emitted by a fire.

Timing and spatial scale	Each of the MODIS satellites (Aqua and Terra) pass overhead approximately twice per day. We analysed the full dataset from the Terra satellite from the start of Jan 2003 to the end of Oct 2023.
Data exclusions	In the main analysis, we did not analyse data prior to the year 2003 because the 2003 was the first year both the Terra and Aqua satellites were both operational for full years. We excluded locations labelled as likely resulting from non-fire sources, such as volcanoes, other static sources, or offshore (e.g., industrial). For additional robustness, we further filtered out "low confidence" fires (i.e., confidence < 30). We also excluded hotspots that were likely duplicated as a result of overlapping swaths of successive satellite overpasses. Polar orbiting satellites are biased at high latitudes because there is some overlap in the swaths of adjacent satellite overpasses, leading to the possibility that the same pixel is double counted in subsequent orbits. We attempted to correct this problem by identifying and omitting likely duplicate hotspots. For the Terra and Aqua satellites, there should each be a maximum of one hotspot for each day and each night in each pixel. Thus, to identify likely duplicates, we identified pixels with multiple observations in a given day or night at a resolution of 500 m. Such cases with multiple hotspots indicate a likely duplicate, in which cases we retained one hotspot at random, leaving a combined maximum of four hotspots per 24-h period in each location. Of a total dataset of 88.4 million hotspots, this cleaning process removed 176,181 (0.19%) likely duplicates.
Reproducibility	The analysis is fully reproducible. Data are from a standardized, permanent, public source. The computer code and data used for analysis have been archived at a permanent repository.
Randomization	N/A
Blinding	N/A

Did the study involve field work? ☐ Yes ☒ No

Reporting for specific materials, systems and methods

We require information from authors about some types of materials, experimental systems and methods used in many studies. Here, indicate whether each material, system or method listed is relevant to your study. If you are not sure if a list item applies to your research, read the appropriate section before selecting a response.

Materials & experimental systems

n/a	Involved in the study
☒	☐ Antibodies
☒	☐ Eukaryotic cell lines
☒	☐ Palaeontology and archaeology
☒	☐ Animals and other organisms
☒	☐ Clinical data
☒	☐ Dual use research of concern
☒	☐ Plants

Methods

n/a	Involved in the study
☒	☐ ChIP-seq
☒	☐ Flow cytometry
☒	☐ MRI-based neuroimaging

Plants

Seed stocks	N/A
Novel plant genotypes	N/A
Authentication	N/A